10A.1

TROPICAL CYCLONE FORMATION: A SYNOPSIS OF THE SYSTEM-SCALE DEVELOPMENT

Kevin J. Tory[1]
Centre for Australian Weather and Climate Research, Melbourne, Australia

Michael T. Montgomery
Naval Postgraduate School, Monterey California and NOAA Hurricane Research Division, Miami Florida

1. Introduction

Tropical Cyclone (TC) formation can be regarded as a two-stage process in which (i) the atmosphere becomes favorable for development, and (ii) the TC-scale warm-core troposphere-deep vortex develops. This paper addresses the second stage, focusing on the system-scale. We assume (i) that a synoptic-scale area of enhanced vertical component of absolute vorticity (ζ_a) exists in the lower to middle troposphere of a tropical oceanic environment; (ii) a sub-area semi-protected from low- to middle troposphere lateral flow is present within this region, and (iii) the sub-area is convectively active for a sustained period of time. We describe a system scale intensification process consistent with recent modeling studies (Hendricks et al. 2004; Montgomery et al. 2006; Tory et al. 2006a, b, 2007; Nolan 2007).

Because TCs are defined by their wind characteristics we choose to describe the formation process in terms of the wind dependent parameter ζ_a. In section 2 vorticity conservation arguments (Haynes and McIntyre 1987, hereafter HM87) are used to describe cloud- and system-scale vorticity concentration. Section 3 discusses the changing thermodynamic conditions that increase the efficiency of the system-scale in-up-out secondary circulation, and section 4 describes the non-linear increase in system-scale spin-up efficiency.

2. Insight from vorticity theory

The ζ_a tendency can be expressed in flux form following HM87,

$$\frac{\partial \zeta_a}{\partial t} = -\nabla.\left[(u,v,0)\zeta_a + \omega\frac{\partial}{\partial p}(v,-u,0)\right], \qquad 1$$

where u and v are the wind components parallel to pressure surfaces, ω represents the flow perpendicular to pressure surfaces, and p is pressure. (Frictional forces are neglected.) Integrating Eq. 1 over an arbitrary volume (V) and using the divergence theorem to express the term on the RHS of Eq. 1 as a surface integral, the net ζ_a tendency inside the volume becomes,

$$\iiint_V \frac{\partial \zeta_a}{\partial t} dV = -\iint_S \left[\vec{J}_a + \vec{J}_\omega\right]\hat{n}dS, \qquad 2.$$

$$\vec{J}_a = (u,v,0)\zeta_a \text{ and } \vec{J}_\omega = \omega\frac{\partial}{\partial p}(v,-u,0).$$

Here $\hat{n}$ is a unit vector normal to the surface S. $\vec{J}_a.\hat{n}$ and $\vec{J}_\omega.\hat{n}$ represent the advective and non-advective ζ_a fluxes through S respectively. The latter flux was labeled non-advective by HM87 because it does not represent a physical ζ_a transport, instead it represents a local ζ_a source-sink dipole that can be expressed mathematically as a ζ_a flux. From Eq. 2 there can be no net change in ζ_a

[1] *Corresponding author address*: Kevin J. Tory, BMRC, GPO Box1289K, Melbourne, Australia, 3001. Email: k.tory@bom.gov.au

within any volume bounded by a surface in which the ζ_a fluxes normal to the surface are everywhere zero. Because the vertical component of both fluxes is zero, the normal component to all pressure surfaces is zero, which gives rise to the HM87 statement that there can be no net change in ζ_a between pressure surfaces. (This is true when friction and diabatic heating is included, for non-hydrostatic flows, and for PV on isentropic surfaces (HM87).)

The conservation arguments are also true for $\vec{J}_a$ and $\vec{J}_\omega$ independently. For example, on any closed lateral surface in which $\vec{J}_a.\hat{n}$ is everywhere zero, there can be no net change in ζ_a from advective tendencies within the contained volume. The same is true for $\vec{J}_\omega$. Two trivial examples of zero flux surfaces are surfaces of zero flow[2], i.e., $\vec{u}=0$ and $\omega=0$ for $\vec{J}_a$ and $\vec{J}_\omega$ respectively. The latter example gives rise to the statements of Tory et al. (2008) that the net $\vec{J}_\omega$ tendency is zero between pressure surface layers within updrafts and downdrafts (where the updraft and downdraft surfaces are defined by $\omega=0$, and the pressure surface layers do not intersect a boundary). Any local source-sink ζ_a dipoles that result from the non-advective tendency must be entirely contained within updrafts and downdrafts. These additional conclusions are also true for PV on isentropic surfaces. The ζ_a tendencies are illustrated schematically in Fig. 1.

The intensification of ζ_a during TC formation can only come about from a reorganization of existing ζ_a between pressure surfaces; ζ_a at one pressure level cannot be sourced from another level[3]. Figure 1 gives a schematic illustration of the advective and non-advective ζ_a tendencies. Inside the surface of $\vec{J}_a.\hat{n}=0$ (upper panel) there is no net change in ζ_a from advective tendencies. However, there are local changes within, positive tendencies where the flow is convergent and negative where it is divergent. This is illustrated by the advective ζ_a flux vector $\vec{J}_a$. In the lower panel two updrafts and a downdraft are depicted embedded in the convergent flow. Analogous to the advective flux, there is no net change in ζ_a from non-advective tendencies within the surfaces of $\vec{J}_\omega.\hat{n}=0$, but local changes introduce a ζ_a tendency dipole, illustrated by the non-advective ζ_a flux vector, $\vec{J}_\omega$.

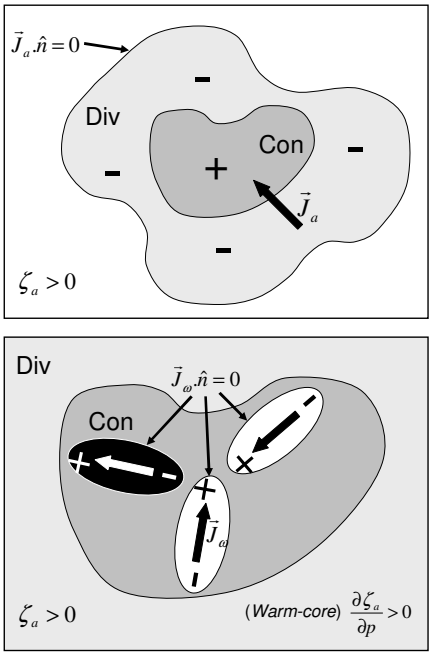

Figure 1: Horizontal schematic of advective (upper) and non-advective (lower) ζ_a tendency. (The lower panel is a sub-domain of the upper panel.) The pale and dark shading represent regions of net divergence and convergence respectively. The + and – symbols indicate positive and negative ζ_a tendency. In the upper panel the outer surface encloses an area of zero net-convergence ($\vec{J}_a.\hat{n}=0$). The thick arrow represents the advective ζ_a flux vector, $\vec{J}_a$. The lower panel illustrates a distribution of vertical motion (updrafts white, downdraft black) within the convergent region. The thick arrows represent the non-advective ζ_a flux vector, $\vec{J}_\omega$ for a warm-cored NH background circulation. (Because $\partial\zeta_a/\partial p>0$ the updraft gives an inward $\vec{J}_\omega$ flux.)

[2] The surface of zero flow can be relative to a moving reference frame.

[3] Vertical PV projection (e.g., Hoskins et al. 1985) does not involve cross-isentropic PV transport. Instead flow changes are induced that concentrate or dilute PV within isentropic surfaces.

While the Fig. 1 schematic shows $\vec{J}_{\omega}$ contributes no net ζ_a change in the up- and downdrafts, and hence no net ζ_a change in the central convergent region, sufficiently intense anomalies can in time migrate inwards and outwards and thus increase the contribution from the advective tendency, i.e., a distinct "eddy contribution" to the system-scale spin-up. In general cyclonic vorticity anomalies migrate towards increasing cyclonic vorticity, and anticyclonic anomalies migrate towards decreasing cyclonic vorticity (McWilliams and Flierl 1979, Smith and Ulrich 1990, Montgomery and Enagonio 1998, Schechter and Dubin 1999). The effect of this vorticity segregation process enhances the existing background vorticity gradient. The anomalous vorticity migration can even be sufficiently robust to proceed against the system mean inflow and outflow (Nguyen et al. 2008). It is of interest to point out that this vortex segregation mechanism provides what we believe to be the most likely explanation for (i) the formation of the upper-level cyclonic TC core that develops in a layer of mean divergent flow, and (ii) large areas of upper-level anticyclonic PV and ζ_a often observed surrounding intensifying TCs (Alaka 1962, Shapiro and Franklin 1995, Molinari et al. 1998, Wu and Chen 1999).

3. Thermodynamic considerations

The mean convergence of environmental ζ_a (Fig. 1 upper panel) is facilitated by the system-scale in-up-out secondary circulation, and provides a significant contribution to the spin-up of the lower troposphere circulation (e.g., Montgomery et al. 2006, Tory et al. 2006b). This in-up-out circulation is driven by system-scale buoyancy forcing due to the release of latent heat in the convective region (e.g., Smith et al. 2005). For the in-up-out circulation to most effectively spin-up the system-scale primary circulation the thermodynamic conditions must favor convection that drives a troposphere-deep vertical mass flux. Evaporation of rain and cloud water can introduce a local downward mass-flux (e.g., convective downdrafts, stratiform subsidence), particularly in the low- to middle-troposphere. On the system-scale this opposition to the net upward mass-flux reduces the lower-level convergent inflow, and consequently the mean system-scale ζ_a concentration. It is also conceivable that a convective region dominated by stratiform precipitation could be divergent in the mean at low-levels, and thus directly spin-down the system-scale primary circulation.

An estimate for the evaporative downdraft potential of a parcel is given by the downdraft convective available potential energy (DCAPE, Emanuel 1994). If rain or cloud water is evaporated into the parcel it will saturate at the parcels, wet-bulb temperature. If evaporation is maximized as the parcel falls it will follow a moist adiabat on a thermodynamic diagram such as the skew-T log-P, or the Australian equivalent F-160 diagram. Fig 2 illustrates a hypothetical parcel path satisfying the above thermodynamic processes on an F-160 diagram. The shaded area represents the parcels DCAPE. The area can be divided into two sub areas, the DCAPE that would be generated if the parcel was initially saturated (labeled saturated DCAPE in Fig. 2), and the remaining area (labeled unsaturated DCAPE).

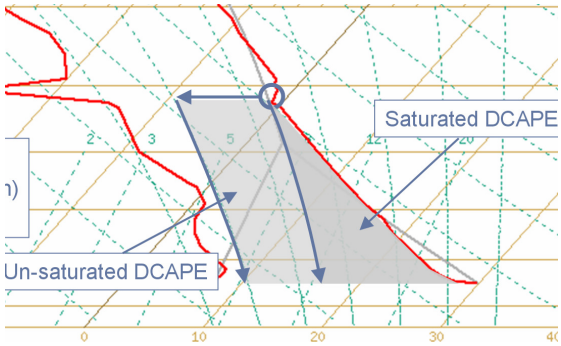

Fig. 2: Downdraft CAPE (Emanuel 1994) as depicted on an F-160 thermodynamic diagram. Red lines represent environmental temperature and dew-point temperatures. See the text for an explanation for the DCAPE sub-division.

This sub-division is important for illustrating processes required to reduce DCAPE. It can be seen from the figure that moistening of the convective region environment reduces the un-saturated DCAPE, and stabilization of the environment below the parcel reduces the saturated DCAPE. Persistent convection both moistens and stabilizes through mixing between updrafts and downdrafts and their immediate environment. It follows then that for a somewhat contained region of persistent convection (i.e., protected from dry air intrusions or leakage of moist air), the lower- to middle-troposphere will both moisten and stabilize with time, and the downdraft mass-flux will decrease with time. This transition will increase the efficiency of the mean in-up-out circulation and consequently the system-scale spin-up efficiency.

Earlier concerns that downdrafts generally inhibit TC formation by removing conditional instability when low-entropy air is transported to the surface from mid-levels (e.g., Bergeron 1950, Rotunno and Emanuel 1987), may be overemphasized. Surface observations from tropical oceanic MCSs show a mix of high and moderately low entropy (Kingsmill and Houze 1999), and modeling studies suggest downdraft gust fronts may in fact invigorate convection when high entropy air is lifted sufficiently while interacting with the denser flow.

4. Non-linear growth in development efficiency

Solutions to the Eliassen (1951) balanced vortex model show that a point heat source in a rotating stratified environment induces a toroidal secondary circulation with vertical motion concentrated in the vicinity of the heat source and broader subsidence distributed at larger radii. The inflow and outflow spin-up and spin-down the primary circulation respectively. The vertical flows outside the point heat source introduce adiabatic warming and cooling that provides a pressure gradient that balances the changes in primary circulation. This is depicted schematically in Fig. 3. The stronger the static (N) and inertial (I) stabilities, the smaller the vertical and horizontal displacements required to introduce a given change in pressure gradient and primary circulation respectively. Thus the geometry of the secondary circulation is dependent on the ratio of inertial to static stabilities.

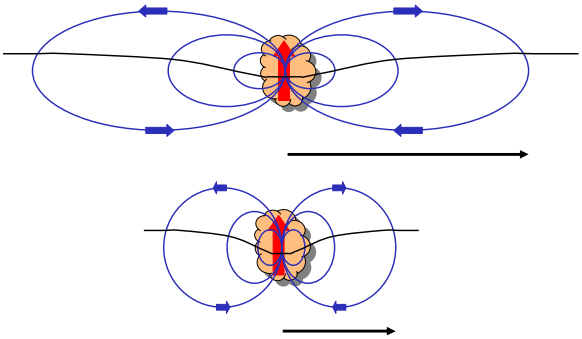

Figure 3: A schematic representation of the secondary circulation (blue streamlines) induced by a point heat source (orange) following Eliassen (1951), for a relatively weak (upper) and strong (lower) background circulation. The black line represents an isentrope perturbed by the secondary circulation and the black arrow represents the Rossby radius, L_R.

In the real atmosphere the heating is finite (provided by an ensemble of convective elements), the vertical circulation is confined to the troposphere, static stability changes are small compared with inertial stability changes, and the atmosphere evolves towards a state of balance (rather than evolves in a balanced state). As a first approximation we can assume axisymmetry, and the secondary circulation geometry is determined from the Rossby radius of deformation (L_R). Where,

$$L_R = \frac{NH}{I},\ I = \sqrt{\zeta_a\left(f + 2\frac{v}{r}\right)}, \text{ and}$$

$$\zeta_a = f + \frac{1}{r}\frac{\partial rv}{\partial r}.$$

H is the troposphere depth, ζ_a is the axisymmetric vertical component of absolute vorticity, f is the Coriolis parameter, v is the tangential wind (primary circulation), and r is the radial distance from the circulation centre. The tendency of v and ζ_a are proportional to the product of ζ_a and the inflow and convergence respectively, i.e.,

$$\frac{\partial v}{\partial t} \propto -u\zeta_a, \text{ and } \frac{\partial \zeta_a}{\partial t} \propto C\zeta_a, \quad 3., 4.$$

where u is the radial wind and C is the horizontal convergence. Gradient wind balance is given by,

$$\frac{1}{r}\frac{\partial p}{\partial r} = fv + \frac{v^2}{r},$$

where p is pressure.

For a weak circulation I is small and L_R is large, and convective heating induces a broad secondary circulation with only small changes in v and a small balancing pressure gradient. The dependence on the secondary circulation scale on L_R becomes intuitive when continuity is considered. The upward mass flux must be balanced by subsidence, and for a weak circulation the subsidence must be spread over a large area, otherwise it will introduce a pressure gradient in excess of that needed to balance the weakly enhanced v. Whereas, for an intense circulation with large v and ζ_a, a small radial inflow induces a large increase in v that must be balanced by a strong change in pressure gradient. This requires a greater magnitude of subsidence locally, and because the downward mass flux is finite the subsidence is concentrated over a smaller area. This is consistent with the reduction in L_R.

The axisymmetric balanced response of a circulation to local heat and momentum sources can also be described by the Sawyer-Eliassen equation for the toroidal streamfunction (e.g., Smith et al. 2005),

$$\frac{\partial}{\partial r}\left[-g\frac{\partial\chi}{\partial z}\frac{1}{\rho r}\frac{\partial\psi}{\partial r}-\frac{\partial(\chi C)}{\partial z}\frac{1}{\rho r}\frac{\partial\psi}{\partial z}\right]+$$

$$\frac{\partial}{\partial z}\left[\left(\xi\chi\zeta_a+C\frac{\partial\chi}{\partial r}\right)\frac{1}{\rho r}\frac{\partial\psi}{\partial z}-\frac{\partial(\chi C)}{\partial z}\frac{1}{\rho r}\frac{\partial\psi}{\partial r}\right]=$$

$$g\frac{\partial}{\partial r}\left(\chi^2\dot{\theta}\right)+\frac{\partial}{\partial z}\left(C\chi^2\dot{\theta}\right),$$

where $\chi=1/\theta$, $\xi=2v/r+f$, $\dot{\theta}=\frac{d\theta}{dt}$ is the diabatic heating rate, and $C=v^2/r+fv$ the sum of the centrifugal and Coriolis forces.

Inside the heating region the falling pressure is facilitated by an excess of diabatic heating over adiabatic cooling (e.g., Shapiro and Willoughby 1982).

In this way the diabatic energy release powers an atmospheric adjustment in the form of a spin-up of the system-scale circulation. The spin-up occurs irrespective of the heat-source scale and the intensity of the background rotation. But as the circulation intensifies the atmospheric adjustment to the diabatic energy release becomes focused within an ever-decreasing volume (i.e., the spin-up energy becomes more and more focused towards the heat source). This is consistent with conclusions from TC intensification studies that the spin-up efficiency, within the vicinity of the heat source, increases with circulation intensity (e.g., Schubert and Hack 1982, Hack and Schubert 1986, Nolan et al. 2007).

5. Summary

The vorticity conservation principles of Haynes and McIntyre (1987) show that the TC vortex construction comes about from a reorganization of existing ζ_a between pressure surfaces. The mean in-up-out circulation in a convective complex concentrates environmental ζ_a, which contributes to a substantial low-level intensification of ζ_a.

The mean in-up-out circulation in the convective complex is driven by diabatic heating in an ensemble of convective elements. The heating introduces an upward buoyancy force that drives a net upward mass flux, which is accompanied by a return circulation with outflow above, inflow below, and subsidence at some greater distance. Evaporation of rain or cloud water can introduce downdrafts, particularly in the low- to middle troposphere, that oppose the upward mass flux and thus weaken the low-level convergence and potential for the system to spin-up the low-level circulation. The potential for downdrafts can be represented by DCAPE on a thermodynamic diagram. Both moistening of the low- to middle-troposphere, and stabilization of the lower troposphere reduces DCAPE. Convective processes (e.g., convective updrafts and downdrafts, stratiform subsidence, entrainment and detrainment) facilitate both the moistening and stabilization.

Thus, in a region somewhat protected from lateral flows, persistent convection will, given sufficient time, create an environment that supports deep convection on a scale of hundreds of km. This is likely to give the Eliassen mechanism sufficient impetus to begin the non-linear intensification of the system as a whole. Provided convection is maintained on a sufficient scale and remains protected from lateral intrusions of dry air, the Eliassen mechanism alone will lead to a non-linear amplification of the system-scale primary circulation. Note that while heat and moisture fluxes from the sea surface are still required to maintain the convection by replenishing boundary layer θ_e, recent work has demonstrated that the non-linear amplification requires no feedback between the wind speed and surface fluxes (e.g., Nguyen et al. 2008). This is contrary to the wind induced surface heat exchange (WISHE) theory (Yano and Emanuel 1991, Emanuel et al. 1994), in which a positive feedback between the surface fluxes and wind speed are said to be essential for intensification. This mechanism has the potential to intensify the system well beyond the point in which it becomes self-sustaining.

Acknowledgements

This work has benefited from very useful discussions with our colleagues Noel Davidson and Jeff Kepert.

References

Alaka, M. A., 1962: On the occurrence of dynamic instability in incipient and developing hurricanes. *Mon. Wea. Rev.*, **90**, 49—58.

Bergeron, T., 1950: ¨Uber der mechanismus der ausgiebigan niederschl¨age. *Ber. Dtsch. Wetterd.*, **12**, 225-232.

Eliassen, A., 1951: Slow thermally or frictionally controlled meridional circulation in a circular vortex. *Astrophys. Norv.,* **5,** 19–60.

Emanuel, K. A., 1994: Atmospheric convection. *Oxford University Press.*

Emanuel, K. A., J. D. Neelin and C. S. Bretherton, 1994: On large-scale circulations in convecting atmospheres. *Quart. J. Roy. Meteor. Soc.*, **120**, 1111—1430.

Hack, J. J., and W. H. Schubert, 1986: Nonlinear response of atmospheric vortices to heating by organized cumulus convection. *J. Atmos. Sci.,* **43,** 1559–1573.

Haynes, P. H. and M. E. McIntyre, 1987: On the evolution of vorticity and potential vorticity in the presence of diabatic heating and frictional or other forces. *J. Atmos. Sci.*, **44**, 828—841.

Hendricks, E. A., M. T. Montgomery and C. A. Davis, 2004: On the role of "vortical" hot towers in hurricane formation. *J. Atmos. Sci.,* **61**, 1209—1232.

Hoskins, B. J., M. E. McIntyre and A. W. Robertson, 1985: On the use and significance of isentropic potential vorticity maps. *Quart. J. Roy. Meteor. Soc.* **111**, 877—946.

Kingsmill, D. E. and R. A. Houze Jr., 1999: Thermodynamic characteristics of air flowing into and out of precipitating convection over the west Pacific warm pool. *Quart. J. Roy. Meteor. Soc.* **125**, 1209—1229.

McWilliams, J. C., and G. R. Flierl, 1979: On the evolution of isolated nonlinear vortices. *J. Phys. Oceanogr.*, **9**, 1155 - 1182.

Molinari, J., S. Skubis, D. Vollaro and F. Alsheimer, 1998: Potential Vorticity Analysis of Tropical Cyclone Intensification. *J. Atmos. Sci.,* **55**, 2632—2644.

Montgomery, M. T. and J. Enagonio, 1998: Tropical cyclogenesis via convectively forced vortex Rossby waves in a three-dimensional quasigeostrophic model. *J. Atmos. Sci.*, **55**, 3176—3207.

Montgomery, M. T., M. E. Nicholls, T. A. Cram and A. Saunders, 2006: A vortical hot tower route to tropical cyclogenesis. *J. Atmos. Sci.*, **63**, 355—386.

Nguyen, V. S., R. K. Smith and M. T. Montgomery, 2007: Tropical-cyclone intensification and predictability in three dimensions. In press. *Quart. J. Roy. Meteor. Soc.*

Nolan, D. S., Y. Moon, and D.P. Stern, 2007: Tropical cyclone intensification from asymmetric convection: Energetics and efficiency. *J. Atmos. Sci.*, **64**, 3377—3405.

Nolan, D. S., 2007: What is the trigger for tropical cyclogenesis? *Aus. Met. Mag.*, **56**, 241-266.

Rotunno, R., and K. A. Emanuel, 1987: An Air-Sea Interaction Theory for Tropical Cyclones. Part II: Evolutionary Study Using a Nonhydrostatic Axisymmetric Numerical Model. *J. Atmos. Sci.*, **44**, 542-561.

Schecter, D. A., and D. H. E. Dubin, 1999: Vortex Motion Driven by a Background Vorticity Gradient. *Phys. Rev. Letters*, 2191-2194.

Schubert, W. H., and J. J. Hack, 1982: Inertial stability and tropical cyclone development. *J. Atmos. Sci.,* **39,** 1687–1697.

Shapiro, L. J., and H. Willoughby, 1982: The response of balanced hurricanes to local sources of heat and momentum. *J. Atmos. Sci.,* **39,** 378–394.

Shapiro, L. J. and J. L. Franklin, 1995: Potential vorticity in hurricane Gloria. *Mon. Wea. Rev.*, **123**, 1465—1475.

Smith, R. K., and W. Ulrich, 1990: An analytical theory of tropical cyclone motion using a barotropic model. *J. Atmos. Sci.*, **47**, 1973-1986.

Smith, R. K., M. T. Montgomery and H. Zhu, 2005: Buoyancy in tropical cyclones and other rapidly rotating atmospheric vortices. *Dyn. Atmos. Oceans.*, **40**, 189—208.

Tory, K. J., M. T. Montgomery and N. E. Davidson, 2006a: Prediction and diagnosis of Tropical Cyclone formation in an NWP system. Part I: The critical role of vortex enhancement in deep convection. *J. Atmos. Sci.*, **63**, 3077—3090.

Tory, K. J., M. T. Montgomery, N. E. Davidson and J. D. Kepert, 2006b: Prediction and diagnosis of Tropical Cyclone formation in an NWP system. Part II: A diagnosis of tropical cyclone Chris formation. *J. Atmos. Sci.*, **63**, 3091–3113.

Tory, K. J., M. T. Montgomery and N. E. Davidson, 2007: Prediction and diagnosis of Tropical Cyclone formation in an NWP system. Part III: Developing and non-developing storms. *J. Atmos. Sci* ., **64**, 3195—3213.

Wu, C-C. and H-J Cheng, 1999: An Observational Study of Environmental Influences on the Intensity Changes of Typhoons Flo (1990) and Gene (1990). *Mon. Wea. Rev.*, **127**, 3003—3031.

Yano, J-I. and K. A. Emanuel, 1991: An improved model of the equatorial troposphere and its coupling with the stratosphere. *J. Atmos. Sci* ., **48**, 377—389.